Electronic Supplementary Material (ESI) for Physical Chemistry Chemical Physics.


# Spectroscopic evidence for acid-base interaction driven interfacial segregation

Saranshu Singla,[†,‡] Michael C. Wilson,[†,‡] and Ali Dhinojwala[*,†]

*Department of Polymer Science, The University of Akron, Akron, Ohio 44325-3909, USA*

E-mail: ali4@uakron.edu

[*]To whom correspondence should be addressed
[†]University of Akron
[‡]S.S. and M.C.W. contributed equally to this work.

# Experimental

## Materials

High-purity organic liquids (benzene, acetone, tetrahydrofuran (THF), N,N-dimethylformamide (DMF), and chloroform) were purchased from Sigma-Aldrich (Table S4). All chemicals were used as received. The liquids were used to prepare binary mixtures with different bulk concentrations of acetone-chloroform, THF-benzene, and DMF-benzene by weight (Tables S5-S7).

## SFG Measurements

### Procedure

The equilateral sapphire prisms (used as substrates) for SFG experiments were first heated in a tube furnace at 760°C for at least 2 h followed by sequential sonication in different solvents (toluene, chloroform, acetone, and ethanol) for 1 h each. Then, the sapphire prisms were sonicated in ultrapure water (Millipore filtration system, 18.2 MΩ·cm) and finally plasma sterilized for 5 min to remove any traces of hydrocarbon contaminants. The stainless steel liquid cells used for holding the sapphire prisms were also cleaned using the same protocol as used for sapphire prisms, with the exception of the tube furnace heating. A clean sapphire prism was placed onto the liquid cell with a teflon spacer and held in place by a clamp. A blank scan was collected for each sapphire prism before injecting liquids into the liquid cell to ensure that the sapphire surface was free of any hydrocarbon contaminants and to locate the position of sapphire free-hydroxyl peak (Figure S2). Due to the observed variation in position of the sapphire free-hydroxyl peak, the SFG spectra in the hydroxyl region were plotted as a function of frequency shift (calculated with respect to the position of the sapphire free-hydroxyl peak for a given experiment) instead of wavenumber.[1]

Afterwards, the assembly was placed under vacuum (∼30 min) to get rid of any traces of bound water. Liquid was then injected into the liquid cell and sealed with brass caps.

The setup was then allowed to remain in the hood for ∼30 min before spectra collection, to ensure proper sealing and equilibration. For liquid mixtures, the lowest concentrations of the strongly segregating component were injected first followed by increasing concentrations. The liquid cell was flushed in between concentrations using the weakly adsorbing liquid.

**Laser System**

SFG spectra were acquired using a Spectra Physics laser system, a detailed description provided in previous publications.[2–5] Briefly, it involves the spatial and temporal overlap of a fixed 800 nm visible beam (∼70 $\mu$J energy, 1 ps pulse width, 1 kHz repetition rate, 1 mm diameter) and tunable infrared (IR) beam (∼3.5 $\mu$J energy, 1 ps pulse width, 1 kHz repetition rate, 100-200 $\mu$m diameter). The SFG spectra were collected in total internal reflection (TIR) geometry using equilateral sapphire prisms (15 mm x 15 mm x 15 mm x 10 mm, c-axis ± 2° parallel to the prism face, Meller Optics, Inc.) as substrates, where the incident angle for the IR beam was adjusted to probe the interface between sapphire and different pure liquids and liquid mixtures. The incident angles used in the current study for different liquids and liquid mixtures are given in Tables S4-S7. The incident angle for the visible beam was ∼1.5° lower than that of the IR beam. The TIR geometry offers significant enhancement in SFG signals, however, this enhancement could be uneven across the entire scanning IR wavelength due to variation in refractive index with wavelength. SFG spectra were collected in PPP (P-polarized SFG, P-polarized visible, P-polarized IR) polarization at room temperature for the hydrocarbon (2750-3200 $cm^{-1}$) and hydroxyl (3100-3800 $cm^{-1}$) regions. For the hydroxyl region, two scans were averaged to improve the signal-to-noise ratio. The presented SFG spectra have not been corrected for changes in Fresnel factors and have been fitted using a Lorentzian equation (Equation S1).

$$I_{SFG} \propto | \chi_{NR} + \Sigma \frac{A_q}{\omega_{IR} - \omega_q + i\Gamma_q} |^2 \quad \text{(S1)}$$

In Equation S1, $\chi_{NR}$ describes the non-resonant contribution that does not change with

scanning wavenumber ($\omega_{IR}$). $A_q$, $\Gamma_q$, and $\omega_q$ are the amplitude strength, damping constant (width), and resonant frequency (peak position) of the $q^{th}$ vibrational resonance, respectively.

**Fitting Mixture Spectra**

First, the pure-liquid SFG spectra were fit using Equation S1 with 1 (chloroform and benzene) or 2 (acetone, THF, and DMF) peaks to obtain the average and standard deviation of the peak positions, widths, and amplitudes. To obtain consistent values despite covariance for the average and standard deviations of the different fit parameters, a more rigorous method was used for the bimodal peaks of acetone, THF, and DMF. First, all of the parameters were allowed to vary, and then only amplitudes and $\chi_{NR}$ were allowed to vary with the position and width fixed. Finally, the widths alone were allowed to vary. The average and standard deviations for the peak position, amplitude, and width were taken from the first, second, and third iterations, respectively. The ratio of the two peaks ($R$) for acetone, THF, and DMF was calculated in order to keep the spectral profile consistent for fitting mixture spectra.

The mixture spectra in the hydroxyl region were fit using three Lorentzian peaks to calculate the relative interfacial concentrations of the two liquids. To determine the values for the peak position and width for chloroform and benzene, the lowest concentration for the particular experiment (0.01 mole % acetone for acetone-chloroform, 0.1 mole % THF for THF-benzene, and 0 mole % DMF for DMF-benzene) was fit as if it were purely chloroform or benzene, but allowing the position and width to vary within the constraint of one standard deviation of the mean for the pure liquids. For the acetone, THF, and DMF, the position, width, $R$, and $\chi_{NR}$ were allowed to vary (in the same manner as pure liquids) for the highest concentration for the particular set of experiments (75 mole % acetone for acetone-chloroform, 100 mole % THF for THF-benzene, and 25 mole % DMF for DMF-benzene). An average of the peak position, width, and $R$ was obtained from the two experimental repeats. Then all mixture concentrations were fit using these parameters from both extremes, only allowing one amplitude factor attributed to each liquid ($A_S$ and $A_W$ for the strongly

and weakly interacting components, respectively) and $\chi_{NR}$ to vary. The interfacial area fraction of the strongly segregating component ($\phi_{S,a}$) was calculated (Tables S8-S10) using the amplitude ratio, as given in Equation S2.

$$\phi_{S,a} = \frac{(R+1) * A_S}{(R+1) * A_S + A_W} \tag{S2}$$

The interfacial area-fractions were converted to interfacial volume fractions ($\phi_{S,m}$) using the area and molar volume for different liquids (Table S11).

# Supplementary Text

## Lifshitz-van der Waals Work of Adhesion

The Lifshitz-van der Waals work of adhesion ($W^{LW}$) can be calculated by Equation S3, where Hamaker constant (H) is calculable from Lifshitz theory (Equation S4) and $d_o$=0.165 nm.[6]

$$W^{LW} = \frac{H}{12\pi d_0^2} \tag{S3}$$

$$H = \frac{3}{4}kT\Big(\frac{\epsilon_1 - 1}{\epsilon_1 + 1}\Big)\Big(\frac{\epsilon_s - 1}{\epsilon_s + 1}\Big) + \frac{3h\nu_e}{8\sqrt{2}}\frac{(n_1^2 - 1)(n_s^2 - 1)}{(n_1^2 + 1)^{0.5}(n_s^2 + 1)^{0.5}[(n_1^2 + 1)^{0.5} + (n_s^2 + 1)^{0.5}]} \tag{S4}$$

In Equation S4, $\epsilon_i$ and $n_i$ represent the dielectric constant and refractive index of liquid (*1*) and substrate ($s$). $\nu_e$ is the absorption frequency of the given liquid, which is available in the literature.[7] $k$ and $T$ are the Boltzmann's constant and temperature, respectively. For sapphire, $\epsilon_s$=9.3 and $n_s$=1.75.[8] The parameters for the liquids are given in Table S11.

## Acid-Base Work of Adhesion

The acid-base work of adhesion ($W^{AB}$) can be calculated by Equation S5, where $n$ is the number of interfacial acid-base pairs and $\Delta H$ is the enthalpy of acid-base interactions.[9] The $n$ used in this work is 9 per nm$^2$, while $\Delta H$ was calculated using the Drago-Wayland and the Badger-Bauer equations.[3,10,11]

$$W^{AB} = n * \Delta H \tag{S5}$$

### Drago-Wayland Equation

Drago and Wayland proposed a four-parameter equation to calculate the enthalpy of interaction ($\Delta H$) using the E and C parameters for the acid and the base (Equation S6).[11] The $E_B$ and $C_B$ parameters have been listed in Table S4 for the liquids used in the present study. The $E_A$ and $C_A$ values of sapphire were taken from Kurian *et al.*[2]

$$\Delta H = E_A E_B + C_A C_B \tag{S6}$$

### Badger-Bauer Equation

In 1937, Badger and Bauer proposed an empirical relationship that relates the enthalpy of mixing ($\Delta$H, kcal/mol) to the shift in the vibrational frequency ($\Delta\nu$, cm$^{-1}$), given by Equation S7.[10,12]

$$\Delta H = m * \Delta\nu \ + \ C \tag{S7}$$

In Equation S7, $m$ and $C$ represent the slope and intercept of enthalpy, $\Delta$H (kcal/mol) vs. frequency shift, $\Delta\nu$ (cm$^{-1}$) plot. The literature reported values of $m$ and $C$ were used for calculating the interaction energies.[2]

### Calculation of the Average Shift for Acetone, DMF, and THF

The hydroxyl regions for acetone, THF, and DMF show bimodal distributions for the sapphire hydroxyl peak. Thus, we use a weighted average of the two peaks to calculate the average sapphire hydroxyl peak position ($\omega_{q,avg}$).

$$\omega_{q,avg} = \frac{A_{q,1} \ * \ \omega_{q,1} \ + \ A_{q,2} \ * \ \omega_{q,2}}{A_{q,1} \ + \ A_{q,2}} \tag{S8}$$

In Equation S8, $\omega_{q,1}$ and $\omega_{q,2}$ are the positions of the two peaks, whereas $A_{q,1}$ and $A_{q,2}$ are the amplitudes of the two peaks. The average peak position ($\omega_{q,avg}$) is subtracted from the frequency of sapphire free-hydroxyl peak ($\omega_{free-OH}$) to calculate the frequency shift, $\Delta\nu$ (Equation S9).

$$\Delta\nu = \omega_{free-OH} \ - \ \omega_{q,avg} \tag{S9}$$

### Calculation of Interaction Parameter, $\alpha$

The interaction parameter ($\alpha$, mJ/mol) was calculated from the Hildebrand solubility parameters of the two liquids ($\delta_1$ and $\delta_2$, $(cal/cm^3)^{0.5}$) in a given mixture (Table S11).

$$\alpha = V * (\delta_1 - \delta_2)^2 * 4186 \tag{S10}$$

In Equation S10, $V$ is the volume of the strongly interacting liquid ($cm^3/mol$) and 4186 is the conversion factor from $cal$ to $mJ$ (Table S11).

**Table S1: Average frequency shift ($\Delta\nu$) for the different liquids. The errors represent ±1 standard deviation.**

| Liquid | Frequency Shift ($\Delta\nu$, $cm^{-1}$) |
|---|---|
| Chloroform | 28±10 |
| Benzene | 56±13 |
| Acetone | 111±9 |
| Dimethylformamide | 113±11 |
| Tetrahydrofuran | 122±9 |

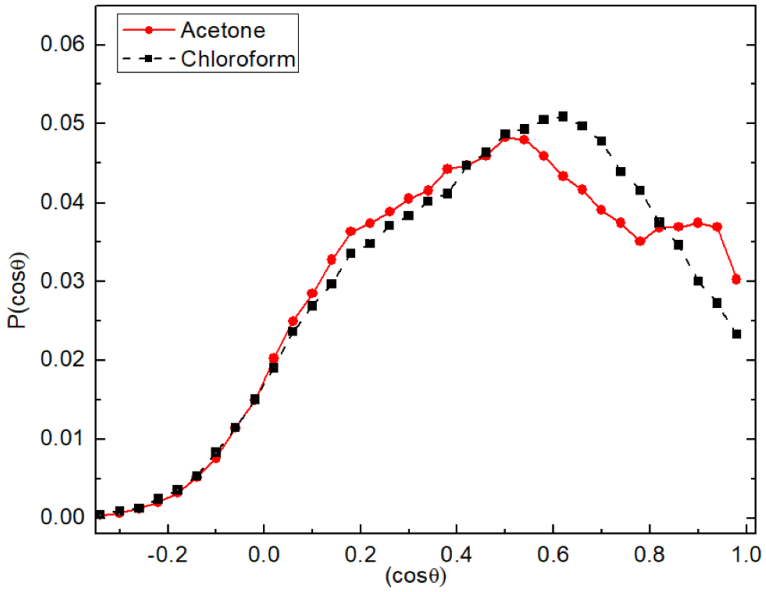


Figure S1: Orientation distribution of sapphire surface hydroxyls with respect to the surface normal for pure acetone (red circles, solid line) and chloroform (black squares, dashed line), respectively.[13] The orientation distribution of sapphire surface hydroxyls does not change significantly with change of liquid next to sapphire.

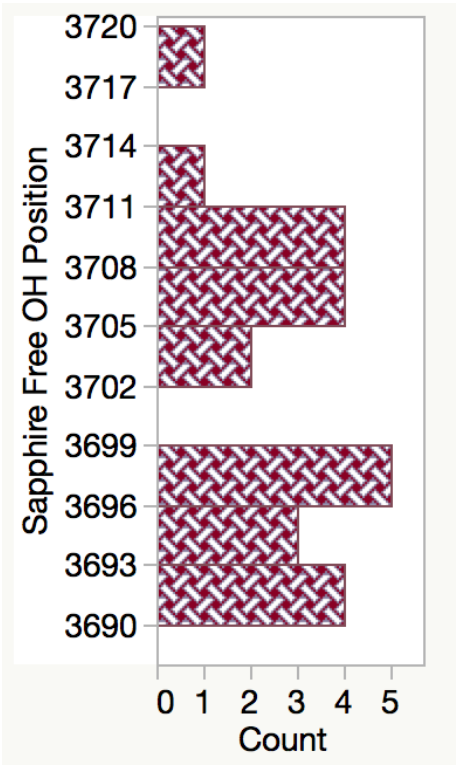


Figure S2: Histogram of sapphire free-hydroxyl peak positions.

**Table S2: Peak assignments in the hydrocarbon region for the different liquids used in the present study.**

| Chemical Name | Peak Position ($cm^{-1}$) | Peak Assignment |
|---|---|---|
| Chloroform[5] | ~3028 | $\nu$(C-H) |
| Benzene[14] | ~3043 | $\nu$(=CH)7a, $\nu$(=CH)7b |
| | ~3073 | $\nu$(=CH)20a, $\nu$(=CH)20b |
| | ~3090 | Comb/Overtone |
| THF[15–17] | ~2875 | $\nu_s$(C-H) |
| | ~2944 | $\nu_a$(C-H) |
| | ~2972 | $\nu_a$(C-H) |
| Acetone[2,18–20] | ~2930 | $\nu_s(CH_3)$ |
| DMF[21] | ~2820 | 1664+1160 |
| | ~2896 | $\nu$(C-H) |
| | ~2945 | $\nu_s(CH_3)N$ |

**Table S3: Components used to calculate the difference in the work of adhesion of the two components ($\Delta W$) using the Fowkes relationship given in Equations 3 and 4.**

| Liquid Mixture | $W_2^{LW}$-$W_1^{LW}$ ($mJ/m^2$) | $W_2^{AB}$-$W_1^{AB}$ ($mJ/m^2$)[a] | $W_2^{AB}$-$W_1^{AB}$ ($mJ/m^2$)[b] |
|---|---|---|---|
| Acetone-Chloroform | 11.2 | -56.6 | - |
| THF-Benzene | -13.6 | -45.0 | -45.69 |
| DMF-Benzene | -6.9 | -38.9 | -55.52 |

[a] Calculated using Badger-Bauer relationship (Equation S7) with $n = 9$ surface hydroxyl groups per $nm^2$, determined using X-ray photoelectron spectroscopy.[3]
[b] Calculated using Drago-Wayland parameters (Equation S6) given in Table S4.

**Table S4: Source, purity, $E_B$ and $C_B$ parameters for all the liquids used in the current study. The last column provides the incident angles used to probe the interface between sapphire and different liquids.[22]**

| Chemical Name | Source | Purity (%) | $E_B$ $(kcal/mol)^{0.5}$ | $C_B$ $(kcal/mol)^{0.5}$ | Incident Angle (°) |
|---|---|---|---|---|---|
| Benzene | Sigma Aldrich | 99.8 | 0.486 | 0.707 | 0 |
| Acetone | Sigma Aldrich | ≥99.9 | 0.987 | 2.33 | 18 |
| THF | Sigma Aldrich | ≥99.9 | 0.978 | 4.27 | 8 |
| DMF | Sigma Aldrich | ≥99.9 | 1.23 | 2.48 | 5 |
| Chloroform | Sigma Aldrich | ≥99.5 | - | - | 6 |

**Table S5: The different bulk concentrations of the acetone-chloroform mixture (given in mole % of acetone) investigated using SFG and the corresponding incident angles used to collect the SFG spectra.**

| Mole % of Acetone (Target) | Mole % of Acetone (Actual) | Incident Angle (°) |
|---|---|---|
| 0.01 | 0.01 | 6 |
| 0.1 | 0.097 | 6 |
| 0.5 | 0.487 | 6 |
| 1 | 0.961 | 6 |
| 5 | 4.614 | 6 |
| 10 | 9.735 | 6 |
| 25 | 23.48 | 6 |
| 50 | 49.96 | 9 |
| 75 | 74.61 | 12 |

**Table S6: The different bulk concentrations of the THF-benzene mixture (given in mole % of THF) investigated using SFG and the corresponding incident angles used to collect the SFG spectra.**

| Mole % of THF (Target) | Mole % of THF (Actual) | Incident Angle (°) |
|---|---|---|
| 0.1 | 0.12 | 0 |
| 1 | 1.07 | 0 |
| 10 | 9.87 | 0 |
| 25 | 23.51 | 0 |
| 50 | 50.80 | 2 |

**Table S7: The different bulk concentrations of the DMF-benzene mixture (given in mole % of DMF) investigated using SFG and the corresponding incident angles used to collect the SFG spectra.**

| Mole % of DMF (Target) | Mole % of DMF (Actual) | Incident Angle (°) |
|---|---|---|
| 0.001 | 0.001 | 0 |
| 0.005 | 0.005 | 0 |
| 0.01 | 0.008 | 0 |
| 0.05 | 0.041 | 0 |
| 0.1 | 0.088 | 0 |
| 0.5 | 0.532 | 0 |
| 1 | 0.935 | 0 |
| 10 | 9.99 | 0 |
| 25 | 25.13 | 0 |

**Table S8: Interfacial area fraction of acetone determined by Equation S2 for acetone-chloroform binary mixtures and calculated bulk and interfacial volume fractions for use in Figure 3.**

| Bulk Volume Fraction ($\phi_{1,l}$) | Interfacial Area Fraction ($\phi_{1,a}$) | Interfacial Volume Fraction ($\phi_{1,m}$) |
|---|---|---|
| 8.90E-05 | 0±0 | 0±0 |
| 8.81E-04 | 0.02±0.04 | 0.03±0.04 |
| 4.45E-03 | 0.30±0.06 | 0.32±0.06 |
| 8.78E-03 | 0.32±0.00 | 0.34±0.00 |
| 4.23E-02 | 0.56±0.01 | 0.58±0.01 |
| 8.96E-02 | 0.56±0.01 | 0.58±0.01 |
| 2.18E-01 | 0.83±0.02 | 0.84±0.02 |
| 4.77E-01 | 0.78±0.01 | 0.79±0.01 |
| 7.28E-01 | 1.00±0.01 | 1.00±0.01 |

**Table S9: Interfacial area fraction of THF determined by Equation S2 for THF-benzene binary mixtures and calculated bulk and interfacial volume fractions for use in Figure 3.**

| Bulk Volume Fraction ($\phi_{1,l}$) | Interfacial Area Fraction ($\phi_{1,a}$) | Interfacial Volume Fraction ($\phi_{1,m}$) |
|---|---|---|
| 1.11E-03 | 0±0 | 0±0 |
| 9.69E-03 | 0.23±0.10 | 0.26±0.11 |
| 9.04E-02 | 0.65±0.01 | 0.65±0.01 |
| 2.18E-01 | 0.83±0.04 | 0.79±0.03 |
| 4.84E-01 | 0.89±0.07 | 0.83±0.06 |

**Table S10: Interfacial area fraction of DMF determined by Equation S2 for DMF-benzene binary mixtures and calculated bulk and interfacial volume fractions for use in Figure 3.**

| Bulk Volume Fraction ($\phi_{1,l}$) | Interfacial Area Fraction ($\phi_{1,a}$) | Interfacial Volume Fraction ($\phi_{1,m}$) |
|---|---|---|
| 8.49E-06 | 0±0 | 0±0 |
| 4.48E-05 | 0.04±0.06 | 0.06±0.08 |
| 6.50E-05 | 0.49±0.09 | 0.56±0.09 |
| 3.55E-04 | 0.66±0.07 | 0.72±0.07 |
| 7.58E-04 | 0.76±0.02 | 0.81±0.01 |
| 4.61E-03 | 0.83±0.05 | 0.87±0.04 |
| 8.10E-03 | 0.89±0.03 | 0.92±0.03 |
| 8.77E-02 | 0.94±0.01 | 0.95±0.01 |
| 2.25E-01 | 0.98±0.03 | 0.99±0.02 |

**Table S11: Parameters used to calculate the different components of the work of adhesion.**

| Parameter | Benzene | Chloroform | Acetone | THF | DMF |
|---|---|---|---|---|---|
| Solubility parameter[a] ($\delta$, $(cal/cm^3)^{0.5}$) | 9.2 | 9.3 | 10.0 | 9.1 | 12.1 |
| Surface tension[a] ($\gamma$, dyne/cm) | 28.9 | 27.16 | 23.3 | 28 | 35 |
| Molar volume[a] ($V$, $cm^3/mol$) | 89.41 | 80.41 | 73.4 | 81.08 | 77.43 |
| Refractive index[a] ($n$) | 1.498 | 1.444 | 1.357 | 1.404 | 1.427 |
| Dielectric constant[a] ($\epsilon$) | 2.28 | 4.8 | 20.6 | 7.6 | 36.7 |
| Molar area ($a$, $10^5$ $m^2/mol$) | 2.90[b] | 2.06[b] | 1.73[b] | 2.19[c] | 1.86[d] |
| Vibrational frequency ($\nu$, $10^{15}$ $s^{-1}$) | 2.1[e] | 2.8[f] | 2.9[e] | 3[f] | 2.6[f] |

[a] Reference[23]
[b] Reference[24]
[c] Reference[25]
[d] Calculated from molar volume
[e] Reference[6]
[f] Reference[7]

## References


(1) Morterra, C.; Magnacca, G. A case study: surface chemistry and surface structure of catalytic aluminas, as studied by vibrational spectroscopy of adsorbed species. *Catal. Today* **1996**, *27*, 497 – 532.

(2) Kurian, A.; Prasad, S.; Dhinojwala, A. Direct measurement of acid–base interaction energy at solid interfaces. *Langmuir* **2010**, *26*, 17804–17807.

(3) Prasad, S.; Zhu, H.; Kurian, A.; Badge, I.; Dhinojwala, A. Interfacial segregation in polymer blends driven by acid-base interactions. *Langmuir* **2013**, *29*, 15727–15731.

(4) Zhu, H.; Jha, K. C.; Bhatta, R. S.; Tsige, M.; Dhinojwala, A. Molecular structure of poly(methyl methacrylate) surface. I. Combination of interface-sensitive infrared-visible sum frequency generation, molecular dynamics simulations, and *ab initio* calculations. *Langmuir* **2014**, *30*, 11609–11618.

(5) Zhu, H.; Dhopatkar, N.; Dhinojwala, A. Effect of acid-base interactions on conformation of adsorbed polymer chains. *ACS Macro. Lett.* **2016**, *5*, 45–49.

(6) Israelachvili, J. N. *Intermolecular and Surface Forces*; Academic press, 2011.

(7) Masuda, T.; Matsuki, Y.; Shimoda, T. Spectral parameters and Hamaker constants of silicon hydride compounds and organic solvents. *J Colloid Interface Sci.* **2009**, *340*, 298–305.

(8) Dobrovinskaya, E. R.; Lytvynov, L. A.; Pishchik, V. *Sapphire: Material, Manufacturing, Applications*; Springer US: Boston, 2009.

(9) Fowkes, F. M.; Mostafa, M. A. Acid-base interactions in polymer adsorption. *Ind. Eng. Chem. Prod. Res. Dev.* **1978**, *17*, 3–7.

(10) Badger, R. M.; Bauer, S. H. Spectroscopic studies of the hydrogen bond. II. The shift of the O–H vibrational frequency in the formation of the hydrogen bond. *J. Chem. Phys.* **1937**, *5*, 839–851.

(11) Drago, R. S.; Wayland, B. B. A double-scale equation for correlating enthalpies of Lewis acid-base interactions. *J. Am. Chem. Soc.* **1965**, *87*, 3571–3577.

(12) Bhatta, R. S.; Iyer, P. P.; Dhinojwala, A.; Tsige, M. A brief review of Badger-Bauer rule and its validation from a first-principles approach. *Mod. Phys. Lett. B* **2014**, *28*, 1430014.

(13) Kumar, N.; Singla, S.; Wilson, M. C.; Kaur, S.; Bekele, S.; Tsige, M.; Dhinojwala, A. Molecular dynamics simulations of acetone-chloroform mixtures on sapphire. *Manuscript in preparation*

(14) Hommel, E. L.; Allen, H. C. The air-liquid interface of benzene, toluene, m-xylene, and mesitylene: a sum frequency, Raman, and infrared spectroscopic study. *Analyst* **2003**, *128*, 750–755.

(15) Evseeva, L. A.; Sverdlov, L. M. Analysis and interpretation of vibrational spectra of tetrahydrofuran and its deutreo derivatives. *Russian Physics Journal* **1968**, *11*, 87–90.

(16) Mizuno, K.; Masuda, Y.; Yamamura, T.; Kitamura, J.; Ogata, H.; Bako, I.; Tamai, Y.; Yagasaki, T. Role of the ether oxygen in hydration of tetrahydrofuran studied by IR, NMR and DFT calculation methods. *J. Phys. Chem. B* **2009**, *113*, 906–915.

(17) Dwivedi, A.; Baboo, V.; Bajpai, A. Fukui function analysis and optical, electronic, and vibrational properties of tetrahydrofuran and its derivatives: a complete quantum chemical study. *Journal of Theoretical Chemistry* **2015**,

(18) Allen, H. C.; Raymond, E. A.; Richmond, G. L. Non-linear vibrational sum frequency

spectroscopy of atmospherically relevant molecules at aqueous solution surfaces. *Curr. Opin. Colloid Interface Sc* **2000**, *5*, 74 – 80.

(19) Yeh, Y. L.; Zhang, C.; Held, H.; Mebel, A. M.; Wei, X.; Lin, S. H.; Shen, Y. R. Structure of the acetone liquid/vapor interface. *J. Chem. Phys.* **2001**, *114*, 1837–1843.

(20) Chen, H.; Gan, W.; Wu, B. H.; Wu, D.; Guo, Y.; Wang, H. Determination of structure and energetics for Gibbs surface sdsorption layers of binary liquid mixture 1. acetone + water. *J. Phys. Chem. B* **2005**, *109*, 8053–8063.

(21) Chalapathi, V. V.; Ramiah, K. V. Normal vibrations of N, N-dimethylformamide and N, N-dimethylacetamide. *Proc. Indian Acad. Sci., Sec. A* **1968**, *68*, 109–122.

(22) Drago, R. S.; Vogel, G. C.; Needham, T. E. Four-parameter equation for predicting enthalpies of adduct formation. *J. Am. Chem. Soc.* **1971**, *93*, 6014–6026.

(23) Smallwood, I. *Handbook of Organic Solvent Properties*; Arnold (Great Britain) and Halsted Press (Americas), 1996.

(24) Webster, C. E.; Drago, R. S.; Zerner, M. C. Molecular dimensions for adsorptives. *J. Am. Chem. Soc.* **1998**, *120*, 5509–5516.

(25) Finley, H. F.; Hackerman, N. Effect of adsorption of polar organic compounds on the reactivity of steel. *J. Electrochem. Soc.* **1960**, *107*, 259–263.